

**POSSIBLE FREQUENCY MODULATION EFFECTS
SINGLED OUT BY THE FOURIER VECTOR AMPLITUDE
IN A $\Delta^{14}\text{C}$ YEARLY SERIES OF GEORGIAN WINES**

ELISABETTA PIERAZZO and SILVIA SARTORI

Dipartimento di Fisica “G Galilei”, Università, I 35131 Padova, Italy
and Laboratori Nazionali INFN, I 35020 Legnaro, Italy

ABSTRACT. The $\Delta^{14}\text{C}$ series of yearly sampled cosmogenic ^{14}C in wines (1909–1952) was analyzed with the Fourier Vector Amplitude (FVA) method, using cyclograms as a graphic tool, to find information on periodicities imprinted by the sun. Because the high sensitivity of the FVA algorithm in detecting periodicities and their variations is emphasized by immediate visualization of its cyclograms, a suggestion has been found for a modulation event. Data are compared with a frequency modulation model, the extension of which to the long 9000–a $\Delta^{14}\text{C}$ series suggests a first approach to interpret the Suess wiggles.

INTRODUCTION

^{14}C is a relatively long-lived cosmogenic radionuclide continuously produced on the earth mainly by the nuclear reaction $^{14}\text{N}(\text{n},\text{p})^{14}\text{C}$ of secondary neutrons on atmospheric nitrogen. The geochemical history of ^{14}C after formation is mixed with the history of the atmospheric carbon, save that ^{14}C decays to the stable ^{14}N by radioactive β decay with half-life $T_{1/2} = 5730 \pm 40$ a.

The order of magnitude of the ratio $^{14}\text{C}/^{12}\text{C}$ in living matter, in equilibrium with atmosphere and hydrosphere, is $\sim 10^{-12}$; its value has slightly changed and fluctuated over the last ten millennia. Our present knowledge of natural ^{14}C variations in terrestrial reservoirs derives from extensive and high-precision measurements of ^{14}C chronology in tree rings; their investigation has also been stimulated by the ^{14}C dating method, one of the basic assumptions of which is the time constancy of terrestrial ^{14}C . However, their understanding is still unsatisfactory.

Carbon reservoir models (Lal & Venkatavaradan, 1970; Oeschger *et al*, 1975; Siegenthaler, Heimann & Oeschger, 1980; Oeschger, 1985) describe the global carbon cycle and interpret the measured CO_2 content of the atmosphere and hydrosphere as dependent on thermodynamic and geochemical parameters of the earth's environment. It is usually assumed that reservoirs are in steady-state equilibrium with the atmosphere, and their ^{14}C content depends both on its influx and exchange; however, Stuiver and Quay (1981) have questioned the steady-state equilibrium over the last 1000 a.

Cosmic-ray (CR) intensity variations at 1 AU (Astronomical Unit is the average distance between the earth and the sun) have been measured in the last half a century; their synoptic view supports the existence of solar-terrestrial relationships. Theoretical models predict modulation of cosmogenic production in the terrestrial atmosphere by interplanetary magnetic fields, controlled by solar activity, and by the geomagnetic field (Lal & Peters, 1962, 1967; Lal & Suess, 1968; Lal & Venkatavaradan, 1970; Castagnoli & Lal, 1980; Stuiver & Quay, 1980a, b; Reedy, Arnold & Lal, 1983a, b).

Forbush (1954, 1966) was the first to point out and measure the inverse correlation between CR intensity and sunspot numbers in cycles #17–18. Eddy (1977) acknowledged periodicity in solar activity through the regular Schwabe cycle of sunspots, which lasts ~ 11 a. Systematic measurements on solar activity – CR flux correlation are available now on several solar cycles (solar cycle # 22 started Sept 1986) (see Shea & Smart, 1988; Iucci *et al*, 1988; Storini, 1989). Analyses of cosmogenic differential reservoirs yield information from the past on CR flux and the periodic or recurrent behavior of the sun.

Variations induced by the geomagnetic field have a time scale of thousands of years; the long-term sinusoidal trend with a period of $\sim 10,000$ a in the 7300-a La Jolla tree rings $\Delta^{14}\text{C}$ (Neffel, Oeschger & Suess, 1981) and in the 8600-a Belfast-Seattle tree rings $\Delta^{14}\text{C}$ (Stuiver, 1989; Pierazzo, 1987) has been generally interpreted as induced by the sinusoidal variation of the earth's dipole field. However, changes in the carbon cycle may be responsible for much of the observed variation in $\Delta^{14}\text{C}$ (Lal & Venkatavaradan, 1970; Lal & Revelle, 1984; Lal, 1985, 1986). Recently, the absence of a similar trend in cosmogenic ^{10}Be in polar ice cast some shadow on the effective influence of the geomagnetic dipole variation (Beer *et al*, 1984, 1988).

The long ^{14}C series in tree rings (Stuiver & Kra, 1986), show common features: the long-period, $\sim 10,000$ a, sinusoidal trend (scale of tens of per mil) and the short-term de Vries variations (Suess wiggles) with a characteristic time scale ~ 100 – 200 a (scale of per mil). The presence of the wiggles has been confirmed in several laboratories and wiggles measured in different series match each other (Sonett & Suess, 1986; Suess, 1986; Finney & Sonett, 1988). Suess (1970, 1980a, b, 1986) has discussed wiggles and described their history as well.

Only decadal or bi-decadal points are available in the atmospheric ^{14}C long series from tree rings. Annual sampling was done only for some periods, due to the limited size of the tree rings and the quantity of wood needed for one conventional radiometric measurement, 30–200g, depending on the wood and chemical procedure (eg, Pearson *et al*, 1977; Stuiver & Quay, 1980b). Future development of accelerator mass spectrometry could reduce the sample size (Wölfli, 1987, 1989).

Wines, whiskies and plant seeds provide annual $\Delta^{14}\text{C}$ series that describe atmospheric ^{14}C . Although some results are still contradictory (Povinec, Burchuladze & Pagava, 1983), solar cycle imprinting has been found in the $\Delta^{14}\text{C}$ series of Georgian wines (Burchuladze *et al*, 1980; Povinec, Burchuladze & Pagava, 1983). Short annual subseries of annual $\Delta^{14}\text{C}$ in tree rings yield similar, though less marked, results (Stuiver & Quay, 1981; Povinec, Burchuladze & Pagava, 1983). Wines are more sensitive than tree rings to solar forcing of cosmogenic production. One point in a $\Delta^{14}\text{C}$ tree-ring series reflects the ^{14}C average concentration during the year, whereas one point in a wine series reflects the concentration during the spring and early summer, when stratospheric-tropospheric mixing is more effective and allows an increase of the cosmogenic concentration in the troposphere. Seasonal variations of tracers in terrestrial reservoirs peaking in the spring-early summer are characteristic of tracers from the

stratosphere (Langway *et al*, 1975); the same holds for cosmogenic concentrations, because the production rate is larger in the stratosphere (Raisbeck *et al*, 1979).

ANALYSIS OF THE DATA

The $\Delta^{14}\text{C}$ yearly series (1909–1952), from Georgian wines kept in the Tbilisi Wine Museum, was reported (Burchuladze *et al*, 1980) and reviewed (Povinec, Burchuladze & Pagava, 1983) along with an analysis of $\Delta^{14}\text{C}$ in tree rings (Stuiver & Quay, 1981) and a comparison with other contemporary $\Delta^{14}\text{C}$ series. The decreasing trend, smaller in wines than in tree rings for the same period (Stuiver & Quay, 1981), was attributed to the Suess effect. Autocorrelation function and spectra of $\Delta^{14}\text{C}$ series of wines and tree rings have shown the 11-a solar cycle (at 95% confidence interval) and its correlation with the solar activity record represented by sunspots, over 4 solar cycles ($\#$ 15–19) with a mean amplitude of $4.3 \pm 1.1\%$ in wines and about half in tree rings.

We have analyzed the Tbilisi wine series for the properties of the Fourier Vector Amplitude (FVA), a high-sensitivity interferential technique that uses cyclograms, and also eyes, to detect periodicities and recurrences of a time series of equispaced data. Recently introduced by M Galli and coworkers in Bologna (Attolini, Cecchini & Galli, 1981, 1983, 1984), the technique is particularly good for picking up imprinting of solar-terrestrial relationships. A comparison between sensitivities – of FVA and of standard spectral analysis – has been carried out in simulated series of sinusoidal modulation events (amplitude modulation (AM) and frequency modulation (FM)) (Pierazzo, 1987).

We ran programs in double precision (64-bit words) on a VAX 8600 of INFN, Padova. We made a normal spectral analysis, detrending the wine series from the Suess effect with a weighted least squares linear fit (Fig 1) and calculating the points $(v_i, P(v_i))$ of the power spectrum (Fig 2) with the Discrete Fourier Transform (DFT). On the abscissae axis of Figure 2 we

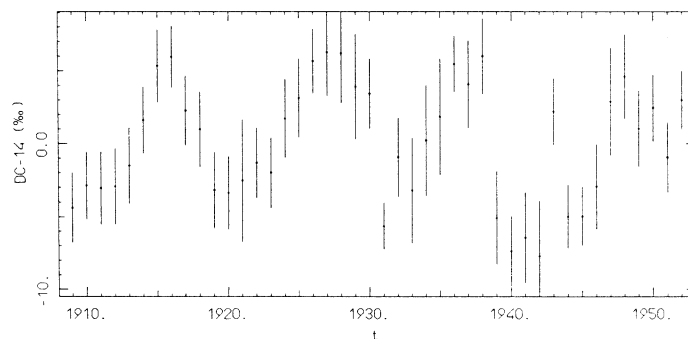


Fig 1. Stationary series of atmospheric $\Delta^{14}\text{C}$ measured in Georgian wines (44 points, 1909–1952) obtained by detrending the data published in Burchuladze *et al* (1980) with a weighted least squares linear fit. There is no visible AM; ~ 2 periods of FM may be present.

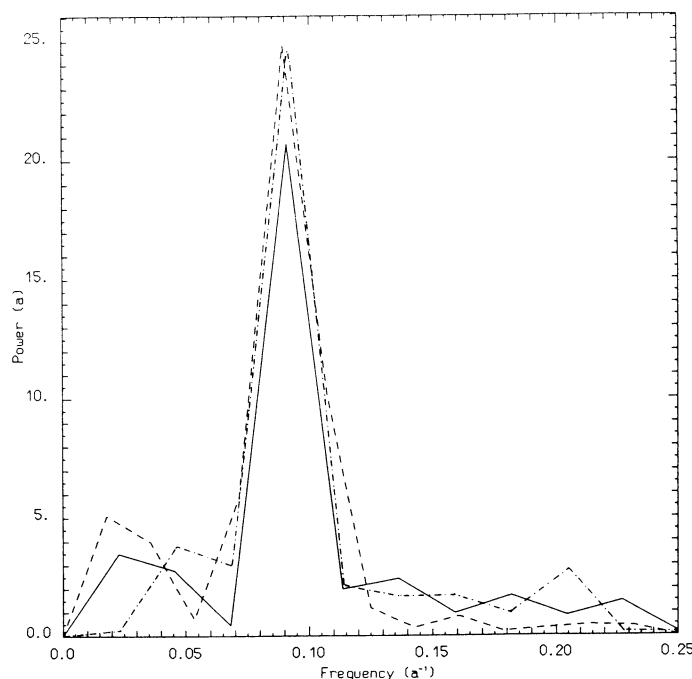


Fig 2. Power spectra of: stationary $\Delta^{14}\text{C}$ wine series (1909–1952) (Fig 1) (—); sunspot numbers (1900–1956) (---); $\Delta^{14}\text{C}$ simulating series (- · - · -), FM model with a small AM component, $T_c = 10.5$, $T_{EM} = 20$, $T_{AM} = 90$ with suitable phases and some noise; see text.

have the continuous frequency ν , expressed in a^{-1} , the SI symbol for year^{-1} . Owing to the DFT's cyclic property, we chose to normalize the sum of the DFT's $P(\nu_i)$ to the total length of the time interval; this roughly corresponds to normalize to 1 the integral of the power continuous curve $P(\nu)$ (the modulus square of the FT of a continuous and infinite time series) on the visible-frequency interval, from 0 to Nyquist frequency ν_N .

We then switched to FVA analysis; we review here the essential features of this rather sophisticated method. The cyclogram is a graphic tool which allows a synoptic understanding of the set of the conventional Fourier amplitudes $a_{\tau,T}$, referring to a given trial period τ , that are obtained by integrating the series on a small window $T \geq \tau$, while the window moves along the series. The amplitudes may be represented as vectors in the complex plane. Moving averages $a_{\tau,T,t}$ are calculated, by averaging the amplitudes $a_{\tau,T}$ on the window T which starts at t , and moving the window T . The vector (1-row matrix) containing the $a_{\tau,T,t}$ set is called the amplitude series; the phase versor series $\alpha_{\tau,T,t}$, also called the phase series, is obtained by the same procedure, after dividing each term of the amplitude series by its modulus.

The cyclograms of the amplitudes and phases are obtained by drawing the polygonal of the vectors $a_{\tau,T,t}$ and $\alpha_{\tau,T,t}$, respectively, starting from the origin (0,0), which corresponds to the beginning of the temporal series.

If the series contains only one periodicity τ_0 , the cyclogram calculated with a trial period $\tau = \tau_0$ goes straight as the window T is moved along the series, whereas cyclograms calculated with $\tau > \tau_0$ or $\tau < \tau_0$ are bent clockwise and counterclockwise, respectively. If the series is long enough, a bent cyclogram may become a circle, the radius of which depends on the difference $\tau - \tau_0$. If more than one periodicity is contained in the series, all cyclograms are bent, except those calculated with the right trial periods, which correspond to the periodicities contained in the series. If there is no periodicity, cyclograms with any trial period go in a random walk.

FVA is a visual computing system (VCS), which uses cyclograms as a graphic tool of a high-sensitivity algorithm, *ie*, a cyclogram easily visualizes the results of the algorithm as an interference between the existing periodicity and a trial period.

Unlike classical spectral analysis, where various detrending, shortening or lengthening of non-stationary series may provide different results (Sonett, 1984), FVA can extract periodicities even in non-detrended series and results are independent of the terminal parts of the series. Moreover, information on the phase of the complex amplitude can be recovered while the integration window moves along the series; thus, the information on temporal evolution of periodicities does not vanish, as it does in conventional spectral analysis.

With the elementary probability theory, we can calculate the probability that a random walk in the (x, y) plane, obtained with n unitary steps, the azimuth of which has a normal Gaussian distribution, reaches a distance R_1 from the origin greater than a fixed quantity d :

$$P(d) = P(R_1 > d) = \exp(-d^2/n).$$

However, this formula is not correct for small values of n and overestimates the real cases, as may be checked by a Monte Carlo simulation; moreover, $P(d)$ must be zero for $d > n$.

When d approaches n , a better approximation to reality (obtained by a Monte Carlo simulation) is made by taking the Fisher transform, z , of the modulus square of the complex correlation coefficient, between the polygonal's versors and versors on the real axis, and approximating its value by its hyperbolic tangent. This substitution has no influence on the probability values for small z , where $\tanh z \approx z$ and the probability is high, whereas, in the neighborhood of the upper limit of R_1 domain, where the probability tends to zero, the new expression is more effective (Attolini, Cecchini & Galli, 1983, 1984; Pierazzo, 1987).

We present a method (Fig 3), integrated over the time series, to recover the best estimate of a periodicity with cyclograms and to evaluate its significance (Pierazzo, 1987; Pierazzo, Sartori & Vanzani, 1988). The choice of the integration window T ($T = 11$, in Fig 3) yields the number of the independent versors of the polygonal (~ 3 for wines, 1909–1952, 44a; ~ 4 for sunspots, 1900–1956, 57a) (Attolini, Cecchini & Galli, 1983, 1984; Pierazzo, 1987). When the abscissa τ varies around the suspected periodicity, the ordinate shows the probability $P(\tau)$ that a polygonal with 3

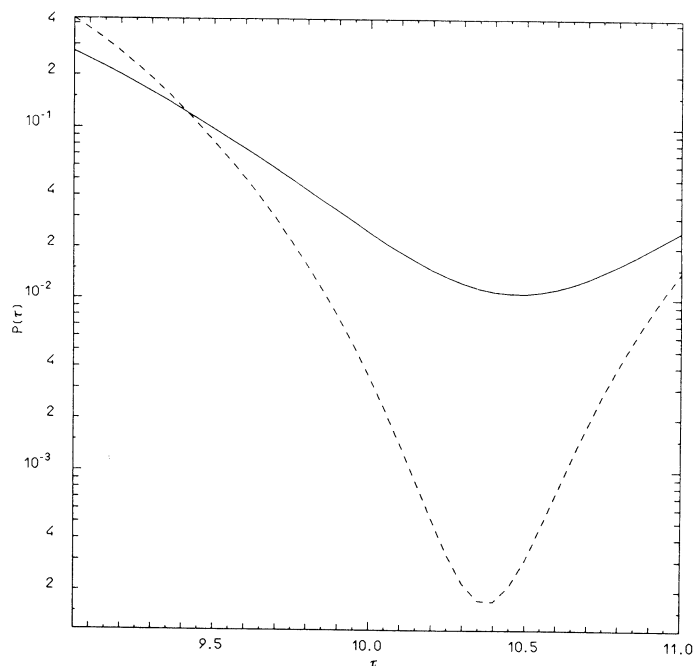


Fig 3. Probability curve $P(\tau)$ of 2-dimensional random paths related to phase-cyclograms, calculated with a trial period τ and moving window $T = 11$, to test the null hypothesis of 2 real series: wines (1909–1952), at least 3 independent versors (—); sunspots (1900–1956), at least 4 independent versors (---). The abscissa corresponding to the minimum is the best estimator for periodicity τ in the series: 10.5 for atmospheric $\Delta^{14}\text{C}$ in wines, 10.4 for sunspots.

(for wines, 4 for sunspots) independent random versors goes farther from the origin than the polygonal referring to the phase-cyclogram, calculated with τ , on the real series. The value of the abscissa where this probability reaches the minimum (10.5 a for the wines, 10.4 a for sunspots) provides a phase-cyclogram with maximum stretching; this value is assumed the best estimate of the periodicity τ contained in the real series. Its position does not depend on the length of the series, whereas a spectral determination does. Its significance against the null hypothesis (random versors) is given by the value of the ordinate; we obtain a probability $1.1 \cdot 10^{-2}$ that a random walk with 3 independent unit vectors would give a walk longer than the walk with $\tau = 10.5$ of the real series of wines, which has 3 independent vectors. Of course, the curve referring to the sunspot record goes deeper: this probability is lower, $1.8 \cdot 10^{-3}$, since it refers to a longer series (4 independent versors).

This method allows us to choose the best value of a periodicity and its significance level in a short interval around the value of the minimum, a rough indication of which is shown by the power spectrum, but does not allow us to choose the minimum on a larger scale. This plot provides a good, though local, evaluation of the periodicity we are looking for, rather independent of the series length, though the method is integrated on the series. If the probability curve shows up several minima, a previous comparison

between cyclograms is needed. Although the cyclogram behavior for a given τ does not depend on the window T ($T \geq \tau$), the probability $P(\tau)$ depends on T , so that, in comparing cyclograms with different τ , the same T should be used.

The phase-cyclogram of the wine series, calculated with $\tau = 10.5$ shows the features of a FM event (Fig 4). The phase-cyclogram of the sunspot record (1900–1956), calculated with $\tau = 10.4$, is also shown for comparison: its behavior does not suggest modulation.

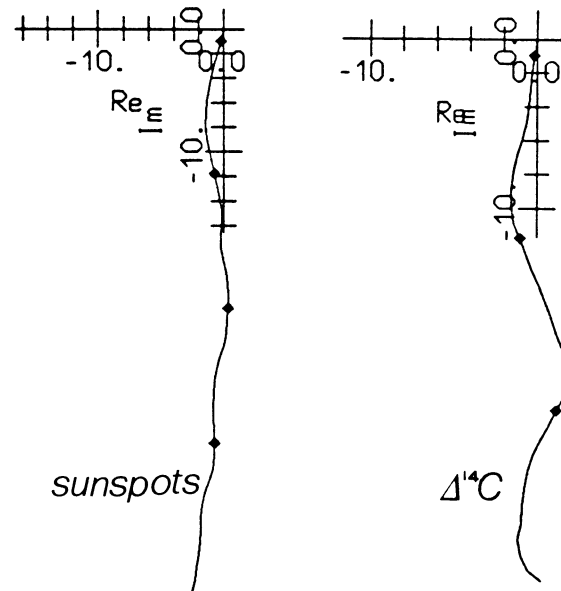


Fig 4. Cyclogram of the $\Delta^{14}\text{C}$ wine series (1909–1952) calculated with the trial period $\tau = 10.5$, corresponding to the minimum of the full curve in Fig 3. Amplitude or frequency modulation may be present, with respect to the carrier frequency $\sim 1/10.5$. Cyclogram of the corresponding sunspot record (1900–1956) calculated with the trial period $\tau = 10.4$, which corresponds to its minimum in Fig 3, is shown for comparison. No suggestion for modulation comes from sunspots.

Spectral analysis (Fig 2) of the wine record shows the 11-a solar peak at $\nu_s = 0.0909 \text{ a}^{-1}$, sharply equivalent to $T_s = 11 \text{ a}$; but ν_s is a multiple of the fundamental frequency $\nu_F = 1/44 \text{ a}^{-1}$, which scans the solar signal with 3 points. Analogously, the peak of sunspot record is shown at $T_s = 11.4$ (the fundamental frequency is $1/57$). However, cyclogram analysis provides $T_s = 10.5 \text{ a}$ for wines and $T_s = 10.4$ for sunspots, with their significance (Fig 3); those values are more precise and are rather independent of the series length and detrending. The best evaluation of the solar cycle in the last century, deduced by spectral analysis on the sunspot record, is $10.6 \pm 0.1 \text{ a}$ (Herman & Goldberg, 1978).

THE FM MODEL

Modulation is usually meant as sinusoidal, in communication engineering. Simulations of (sinusoidal) AM and FM events with carrier and modulating waves of known frequencies have been analyzed with cyclograms (Pierazzo, 1987). We use standard conventions: the index c refers to the carrier wave, frequency ν_c , the index m to the modulating wave, frequency $\nu_m < \nu_c$. To distinguish amplitude modulation from frequency modulation, we also use indices AM and FM for the modulating wave. We show here some basic formulas of modulation of a carrier wave, with angular frequency $\Omega_c = 2\pi\nu_c$ and phase φ_c , by a modulating wave with $\omega_m = 2\pi\nu_m$ and φ_m , respectively.

The AM model is expressed by

$$AM : y(t) = (1 + A \cos(\omega_{AM}t + \varphi_{AM})) \cos(\Omega_c t + \varphi_c)$$

where A is the amplitude modulation index or depth of modulation ($A < 1$); the spectrum shows a peak at the carrier frequency Ω_c , escorted by two lateral peaks at $\Omega_c \pm \omega_{AM}$, the intensity of which depends on A .

The FM model is expressed by

$$FM : y(t) = \cos(\Omega_c t + \varphi_c + B \cos(\omega_{FM}t + \varphi_{FM}))$$

where B is the frequency modulation index; the frequency, $\Omega(t) = 2\pi/T(t)$, is the time derivative of the argument of the cosine

$$\Omega(t) = \Omega_c - B\omega_{FM} \sin(\omega_{FM}t + \varphi_{FM})$$

and varies sinusoidally between $\Omega_c - B\omega_{FM}$ and $\Omega_c + B\omega_{FM}$.

Thus,

$$B = \Delta\Omega/\omega_{FM} \sim (T_{FM}/T_c) (\Delta T/T_c).$$

By developing the previous FM expression (Pierazzo, 1987), we obtain $y(t)$ as a sum of the carrier cosinusoid plus an infinite number of cosinusoids at equispaced frequencies $\Omega = \Omega_c \pm k\omega_{FM}$, with integer k ; each term has a proper coefficient, which is a Bessel function, with a proper index, of the modulation index B . Thus, the spectrum of a FM event consists in a peak at the carrier frequency Ω_c , escorted by two lateral bands containing an infinite number of peaks at $\Omega_c \pm k\omega_{FM}$ with integer k .

In both AM and FM models, line intensities are symmetrical with respect to the central peak, corresponding to the carrier frequency, and the modulating frequency appears as a separation between peaks. In FM, the frequency $\Omega(t)$ varies with modulation index B , but, in the spectrum, only the intensity of the lateral peaks depends on B , whereas their positions depend just on ω_{FM} .

In the analysis of finite length series, at least 2–3 modulation periods should be processed in order to detect the spacing between peaks. In this case, the DFT spectrum represents the Fourier transform of the convolution of the given function with a rectangular window (truncation) representing centering and length of the data series. An asymmetry may be visible

between the left and right bands of the spectrum, if the series does not cover an integer number of FM periods.

The AM model is also represented by the sum of the carrier wave v_c and of the two waves $v_c \pm v_{AM}$; thus, the phase-cyclogram of AM events calculated with a trial period $\tau = T_c$ is a straight line. On the contrary, the phase-cyclograms calculated with $\tau \neq T_c$ are more-or-less complicated, describing ellipses that precede in the plane, sometimes yielding a daisy-like pattern. The maximum stretching for $\tau \neq T_c$ occurs when the trial period corresponds to the two lateral frequencies of the spectrum.

The sum of cosinusoids obtained in a FM model is not so simple as that in AM. Thus, phase-cyclograms of FM events calculated with a trial period $\tau = T_c$ wiggle around a straight line; the wiggle depth is determined by the modulation index B . Maximum stretching occurs at the carrier frequency, yet, unlike AM, no trial period can rectify the cyclogram, since the frequency continuously varies.

The powerful algorithm of FVA detects periodicities with high precision and sensitivity, because it measures, as an interferometric technique, the time between two consecutive crossings of the zero-axis - let us call it a "pseudoperiod", - along the time range of a stationary series. In a FM model, the length of the "pseudoperiod" along the series is not constant and depends on the modulation index B and on the phase φ_{FM} . Thus, the cyclogram calculated with $\tau = T_c$ has wiggles, the depth of which is more or less pronounced, depending on B .

DISCUSSION

The power spectrum of the short atmospheric $\Delta^{14}\text{C}$ record (Fig 2) shows the central peak escorted by two nearly equispaced lateral peaks; this pattern suggests modulation, with $v_m \sim 0.05 \text{ a}^{-1}$ which corresponds to a modulating period $T_m \sim 20 \text{ a}$. Spectral analysis cannot distinguish between AM or FM, because the series is too short.

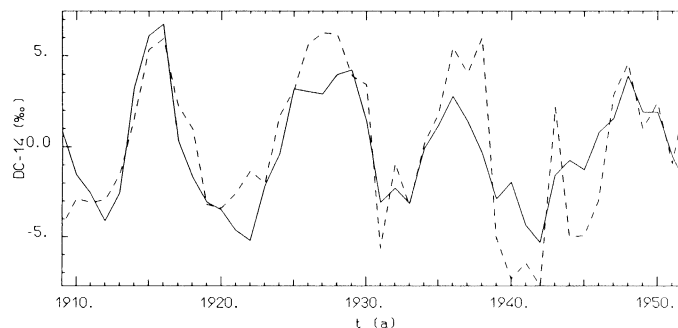


Fig 5. Atmospheric $\Delta^{14}\text{C}$ record from wines (1909–1952) as in Fig 1, without the error bars (---), compared with the yearly series simulated by our FM model with a small AM component, $T_c = 10.5$, $T_{FM} = 20$, $T_{AM} = 90$ with suitable phases, see text (—); some noise has been added to the model to represent a stochastic component.

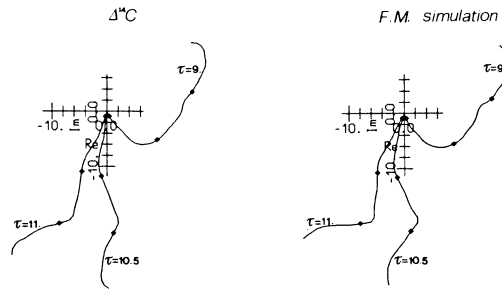


Fig 6. Phase-cyclograms referring to the series shown in Fig 5. Left side: cyclogram of $\Delta^{14}\text{C}$ record with 3 trial periods: $\tau = 10.5$ corresponding to probability minimum of Fig 3, and two values well outside of the minimum: $\tau = 11$, where the probability ratio is ~ 3 , which is very similar to the cyclogram at the probability minimum and $\tau = 9$, where the probability ratio is ~ 20 , which looks different from the cyclogram at the probability minimum. Right side: phase-cyclogram referring to simulated series (FM model with a small AM component, $T_c = 10.5$ $T_{FM} = 20$, $T_{AM} = 90$ with suitable phases and some noise, see text) for the same trial periods. The behavior of the simulated series suggests that the FM model described in the text reproduces the characteristic features of the real $\Delta^{14}\text{C}$ series, stochastic time-behavior apart.

Some hint of FM can be observed in the behavior of the time series and of the cyclograms around the probability minimum, derived from Figure 3. The dashed line linking the experimental points (Fig 5) seems not to cross the zero line with the same period, but with two alternating “pseudoperiods,” the small difference of which suggests a low modulation index B . The phase-cyclogram (Fig 4) calculated with $\tau = 10.5$ (probability minimum of Fig 3 and maximum stretching of the phase-cyclogram) has slight wiggles about a straight line, suggesting again FM with a low modulation index B .

We have tried to reproduce the phase-cyclogram of the measured $\Delta^{14}\text{C}$ in wines with a FM model which could perform ~ 2 modulation periods in the 44-a observed record. We have assumed as carrier period $T_c = 10.5$ a (probability minimum of Fig 3, maximum stretching of the phase-cyclogram and in the FM model); we determined the phase of the carrier sinusoid with the starting phase-angle of the cyclogram, so that the real and the simulated cyclograms have the same straight line to wiggle about. A good choice for the modulating period was $T_{FM} = 20$, as was also roughly suggested by the spectrum (Fig 2); we adjusted the phase of the modulating component to give the simulated series the same wiggling phase like the real one. This simple model reproduces the real cyclogram fairly well (Fig 6). To simulate stochastic components in the measurements, we have also added some noise – in practice, a pseudorandom variable, $RNDM(-1, +1)$, computer-generated in a 64-bit seed – with suitable intensity.

We then added an AM component, with $T_{AM} = 90$ a, (FM \times AM), analogous to the Gleissberg cycle, which modulates the sunspot record; this last improvement was unnecessary in the short record of wines we have processed, which covers only half the AM cycle. To extend our model to a longer period, we added the AM to represent a possible physical solar cycle which could modulate the amplitude of cosmogenic production and be

present beside the Gleissberg cycle (Gilliland, 1981). The mixed FM–AM model we obtained is

$$-4.5 \cos\left(\frac{2\pi t}{10.5} + 0.8 \cos\left(\frac{2\pi t}{20} + \frac{\pi}{10}\right)\right) \left(1 + 0.2 \cos\left(\frac{2\pi t}{90} - 0.37\pi\right)\right) + 4\text{RNDM}(-1, +1)$$

FM ($T_c = 10.5$, $T_m = 20$) × AM ($T_m = 90$) + noise

and is shown with a full line in Figure 5; its spectrum is shown in Figure 2. The FM index we have found, $B = \Delta\omega/\omega_{FM} = 0.8$, allows T to vary between 7.4 a and 18.1 a, in fair agreement with the range of sunspot periods (Eddy, 1977), defined as the intervals between sunspot minima.

Figure 6 shows the phase-cyclograms for the real $\Delta^{14}\text{C}$ record and for the simulated record, calculated with three trial periods: $\tau = 9, 10.5, 11$ a; $\tau = 10.5$ corresponds to the probability minimum for the $\Delta^{14}\text{C}$ record (Fig 3) and the cyclogram is the same as in Figure 4. The other two values were chosen well outside of the minimum: for $\tau = 11$, where the probability ratio is only ~ 3 , the stretching is very similar to the phase-cyclogram stretching at the probability minimum. The cyclogram for $\tau = 9$, where the probability ratio is ~ 20 , looks different from the cyclogram at the probability minimum. The behavior of the phase-cyclogram of the simulated series suggests that the simple FM model and the mixed FM–AM model reproduce the characteristic features of the real $\Delta^{14}\text{C}$ series, in the considered half a century, whereas the stochastic component causes only slight random deviations of the cyclogram from a cyclogram without noise.

We then extended the mixed FM–AM model of atmospheric $\Delta^{14}\text{C}$ to a longer period in the past, to compare its predictions with the real atmospheric $\Delta^{14}\text{C}$ series which spans ~ 9000 a (6650 BC – AD 1910) and is bi-decadal (Pierazzo, 1987). The model was sampled with $\Delta t = 1$ and the resulting points were averaged on contiguous 20-a intervals. Figure 7 presents the bi-decadal model without noise and with two choices of noise, at the same amplitude, only for AD years. The extension to 6650 BC looks similar, showing the nearly regular structure of the ~ 200 a wiggles, which were generated by aliasing.

When a bi-decadal record is obtained from an annual record, the Nyquist frequency ν_N is shifted from 0.5 to 0.025; thus, the peak at $\nu_c = 0.09524$ corresponding to the carrier solar period we have put in the model, $T_c = 10.5$ a, is no longer visible. However, aliasing moves the position of signal lines, hidden behind the Nyquist frequency, from the semiaxis of $\nu > \nu_N$ to the interval $0 < \nu < \nu_N$, which is the visible-frequency domain. Thus, we should find the solar signal (or the remains of it after averaging attenuation) at a position in the low-frequency domain, which is predictable with a simple formula, $\nu = |4\nu_N - \nu_c| = 0.1 - 0.09524 = 0.00476$. By using the equivalent formula for the periods

$$T = \frac{T_c \Delta t}{|kT_c - \Delta t|}$$

since the carrier period is $T_c = 10.5$ and the averaging interval is $\Delta t = 20$, we obtain the aliased period $T = 210$ (or $\nu = 0.00476$). Power spectrum of the simulated series has a very sharp peak at this value, but no visible lateral peaks, that are aliased on the same value of the aliased carrier peak, because in our model $\nu_{FM} = 2\nu_N$.

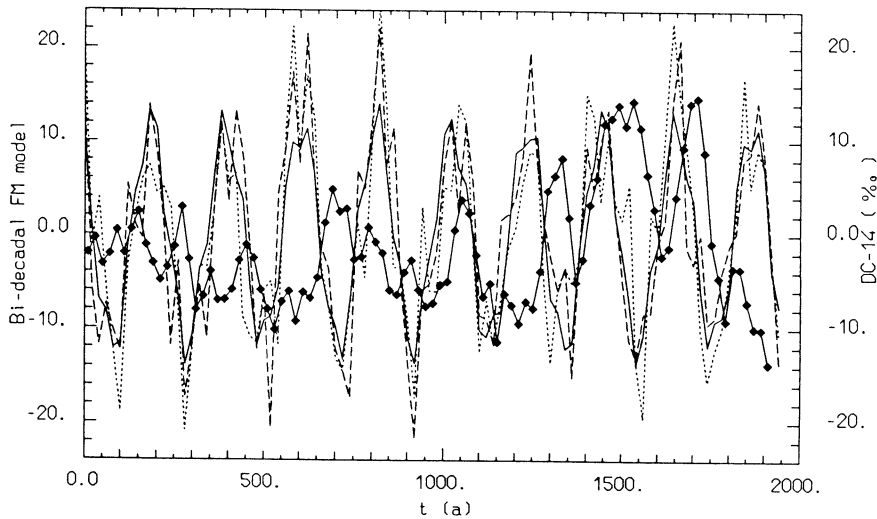


Fig 7. Model prediction on a long bi-decadal atmospheric $\Delta^{14}\text{C}$ record. The FM \times AM model, derived from the short $\Delta^{14}\text{C}$ record in Georgian wines ($T_c = 10.5$, $T_{FM} = 20$, $T_{AM} = 90$ with suitable phases, see text), has been extended to past AD years and arranged to predict the bi-decadal experimental series of atmospheric $\Delta^{14}\text{C}$ (20-a averages on contiguous intervals), made stationary. — = model without noise; \cdots and $---$ = model with 2 choices of noise. \blacklozenge — \blacklozenge — \blacklozenge = experimental $\Delta^{14}\text{C}$ bi-decadal points (Stuiver & Kra, 1986), detrended with a 10,600-a sinusoid (Pierazzo, 1987). Wiggles with time scale of ~ 200 a are evident; they were generated by FM and aliasing. The prediction of $\Delta^{14}\text{C}$ amplitude in the recent past is fairly good. Suess effect is visible in the more recent wiggle. The model also predicts ^{14}C maxima over the solar activity minima: Maunder (1645–1715), Spörer (1416–1543), Wolf (early part of 14th century) (see Stuiver & Quay, 1980).

Figure 7 also shows an experimental bi-decadal $\Delta^{14}\text{C}$ series for AD years taken from the detrended (10,600-a sinusoid) ~ 9000 a atmospheric $\Delta^{14}\text{C}$ series in tree rings (Pierazzo, 1987). We dare interpret Figure 7, in the naive hypothesis that carrier and modulating periods and phases were the same as we found in the four solar cycles of wines. This simple model, when extended to the recent past, reproduces, in amplitude and in position, the increased cosmogenic ^{14}C corresponding to the Maunder (1645–1715), Wolf (early part of 14th century) and Spörer (1416–1534 in terms of measured ^{14}C) minima (Stuiver & Quay, 1980b). The last wiggle, ca 1900, of real ^{14}C is lower than the simulated one because of the Suess effect.

We think that the imperfect agreement (Fig 7) between the model and the bi-decadal series (perhaps better in the recent past) is due to 1) the small lever arm, with which the parameters were determined, *ie*, 44 a of data to make predictions on ~ 2000 a; *eg*, the choice $\nu_m = 1/\Delta t$ has caused the pile-up of the side bands upon the frequency corresponding to the aliased carrier period, 210 a, whereas a different value of ν_m should preserve, in part, the FM side-banded pattern, even when aliased; 2) parameters constancy hypothesis; 3) arbitrary detrending with a least squares 10,600-a sinusoid on the whole ~ 9000 a to account for the “geomagnetic-dipole sinusoid” hypothesis.

CONCLUSION

Annual sampling of ^{14}C yields a record of solar activity in the past. Sampling in wines is more effective than in tree rings; unfortunately, this procedure is possible only for the recent past.

FVA provides a very sensitive interferential method for extracting information on periodicities imprinted by solar activity on cosmogenic temporal series measured in terrestrial reservoirs. FVA can follow even a slight variation of periodicity along the time domain of the series, by handling the phases of the complex amplitudes in the frequency domain. A good part of its success is due to the fact that, unlike conventional Fourier analysis, FVA is rather insensitive to detrending, noise and series length; moreover, FVA displays its results by means of cyclograms. FVA – cyclogram coupling provides a powerful, integrated VCS, unrivalled for FM detection.

A FM model could describe the $\Delta^{14}\text{C}$ atmospheric annual record in analyzed wines, on the four solar cycles # 15–18 with a carrier period $T_c = 10.5$ a, modulated in frequency by $T_m = 20$ a. Although we are not unaware that the lever arm on the wine series is small, we have tried to extend this model, suggested by atmospheric $\Delta^{14}\text{C}$ in wines, to the past. We obtain, maybe surprisingly at first, a prediction of the Suess wiggles, as well as the prediction of the increase of cosmogenic ^{14}C content in terrestrial reservoirs during the Maunder, Spörer and Wolf minima, in fair agreement with the measured values.

ACKNOWLEDGMENTS

We would like to thank Pavel Povinec for inviting us to process the wine data. We are grateful to Minze Stuiver and Paula Reimer, University of Washington, Seattle, for sending us the floppy disk of the 9000-a ^{14}C data. Special thanks go to our teacher, Menotti Galli, University of Bologna, Italy, for introducing us to the inexhaustible reservoir of FVA performances. We are truly indebted to Renee S Kra for carefully editing the manuscript. This work was supported by the Italian Ministry of the Education (law 382/80 60%).

REFERENCES

- Attolini, M R, Cecchini, S and Galli, M, 1981, A new algorithm for the search of non-random oscillations in a time series, *in* Internatl cosmic ray conf, 17th, Paris: Conf Papers, v 8, T 5–17, p 202–205.
- 1983, Cyclic variation analysis of time series, *in* Internatl cosmic ray conf, 18th, Bangalore: Conf Papers, v 9, T 6–2, p 441–446.
- 1984, Time series variation analysis with Fourier Vector Amplitude: Nuovo Cimento, v 7C, no. 2, p 245–253.
- Beer, J, André, M, Oeschger, H, Siegenthaler, U, Bonani, G, Hofmann, H, Morenzoni, E, Nesi, M, Suter, M, Wölfli, W, Finkel, R C and Langway, C, Jr, 1984, The Camp Century ^{10}Be record: implications for long-term variations of the geomagnetic dipole moment: Nuclear Instruments & Methods, v B5, p 380–384.
- Beer, J, Siegenthaler, U, Bonani, G, Finkel, R C, Oeschger, H, Suter, M and Wölfli, W, 1988, Information on past solar activity and geomagnetism from ^{10}Be in the Camp Century ice core: Nature, v 331, p 675–679.
- Burchuladze, A A, Pagava, S V, Povinec, P, Togonidze, G I and Usacev, S, 1980, Radiocarbon variations with the 11-year solar cycle during last century: Nature, v 287, p 320–322.

- Castagnoli, G and Lal, D, 1980, Solar modulation effects in terrestrial production of ^{14}C , in Stuiver, M and Kra, R S, eds, Internatl ^{14}C conf, 10th, Proc: Radiocarbon, v 22, no. 2, p 133–158.
- Eddy, J A, 1977, Historical evidence for the existence of the solar cycle, in White, O R, ed, The solar output and its variations: Boulder, Colorado Assoc Univ Press, p 51–71.
- Finney, S A and Sonett, C P, 1988, High resolution spectral analysis of Irish oak radiocarbon record, in Lunar planetary sci conf, 19th, Proc: Houston, LPI/USRA, p 329–330.
- Forbush, S E, 1954, Worldwide cosmic-ray variations 1937–1952: Jour Geophys Research, v 59, p 525–542.
- 1966, Time-variations of cosmic rays, in Flüggé, S, ed, Handbook of physics, vol 49/1: Berlin, Springer, p 159–247.
- Gilliland, R L, 1981, Solar radius variations over the past 265 years: Astrophysical Jour, v 248, p 1144–1155.
- Herman, J R and Goldberg, R A, 1978, Sun, weather and climate: NASA, SP-426, Washington, DC, p 1–294, 307–333.
- Iucci, N, Parisi, M, Storini, M and Villosi, G, 1988, Large-scale interplanetary perturbations and their influence on the galactic cosmic-ray modulation, in Cini Castagnoli, G, ed, Solar-terrestrial relationships and the earth environment in the last millennia, North Holland, Amsterdam: Internatl school of physics “Enrico Fermi,” Proc, p 408–437.
- Lal, D, 1985, Carbon cycle variations during the past 50,000 years: atmospheric $^{14}\text{C}/^{12}\text{C}$ ratio as an isotopic indicator, in Sundquist, E T and Broecker, W S, eds, The carbon cycle and atmospheric CO_2 : natural variations Archean to present: AGU geophys mono 32, p 221–233.
- 1986, Cosmic ray interaction in the ground: temporal variations in cosmic ray intensities and geophysical studies, in Reedy, R C and Englert, P A J, Workshop on cosmogenic nuclides: LPI tech rept 86–06, Lunar Planetary Inst, Houston, p 43–44.
- Lal, D and Peters, B, 1962, Cosmic ray produced isotopes and their application to problems in geophysics, in Wilson, J G and Wouthuysen, S A, eds, Progress in elementary and cosmic ray physics, vol 4: Amsterdam, North Holland, p 1–74.
- 1967, Cosmic ray produced radioactivity on the earth, in Flüggé, S, ed, Handbook of physics, vol 46/1: Berlin, Springer, p 551–612.
- Lal, D and Revelle R, 1984, Atmospheric P_{CO_2} changes recorded in lake sediments: Nature, v 308, p 344–346.
- Lal, D and Suess, H, 1968, The radioactivity of the atmosphere and hydrosphere: Ann Rev Nuclear Sci, v 18, p 407–434.
- Lal, D and Venkatavaradan, V S, 1970, Analysis of the causes of ^{14}C variations in the atmosphere, in Olsson, I U, ed, Radiocarbon variations and absolute chronology, Nobel symposium, 12th, Proc: New York, John Wiley & Sons, p 549–569.
- Langway, C C, Jr, Klouda, G A, Herron, M M and Cragin, J H, 1975, Seasonal variations of chemical constituents in annual layers of Greenland deep ice deposits, in Isotopes and impurities in snow and ice, Grenoble symp, Proc: IAHS Pub no. 118, p 302–306.
- Neftel, A, Oeschger, H and Suess, H E, 1981, Secular non-random variations on cosmogenic ^{14}C in the terrestrial atmosphere: Earth Planetary Sci Letters, v 56, p 127–147.
- Oeschger, H, 1985, The contribution of ice core studies to the understanding of environmental processes, in Langway, C C, Jr, Oeschger, H, Dansgaard, W, eds, Greenland ice core: geophysics, geochemistry, and the environment: AGU geophys mono 33, p 9–17.
- Oeschger, H, Siegenthaler, U, Schotterer, U and Gugelmann, A, 1975, A box diffusion model to study the carbon dioxide exchange in nature: Tellus, v 27, p 168–192.
- Pearson, G W, Pilcher, J R, Baillie, M G L and Hillam, J, 1977, Absolute radiocarbon dating using a low altitude European tree-ring calibration: Nature, v 270, p 25–28.
- Pierazzo, E (ms), 1987, Analisi di serie temporali nella fisica delle relazioni terra-sole: il metodo della Trasformata di Fourier Vettoriale: Thesis, Univ Padova.
- Pierazzo, E, Sartori, S M and Vanzani, V, 1988, Terrestrial impact cratering record revisited by Vector Fourier analysis, in Lunar planetary sci conf, 19th, Proc: Houston, LPI/USRA, p 929–930.
- Povinec, P, Burchuladze, A A and Pagava, S V, 1983, Short-term variations in radiocarbon concentration with the 11-year solar cycle, in Stuiver, M and Kra, R S, eds, Internatl ^{14}C conf, 11th, Proc: Radiocarbon, v 25, no. 2, p 259–266.
- Raisbeck, G M, Yiou, F, Fruneau, M, Loiseaux, J M, Lieuvin, M and Ravel, J C, 1979, Deposition rate and seasonal variations in precipitation of cosmogenic ^{10}Be : Nature, v 282, p 279–280.

- Reedy, R C, Arnold, J R and Lal, D, 1983a, Cosmic-ray record in solar system matter: *Science*, v 219, p 127–135.
- 1983b, Cosmic-ray record in solar system matter: *Ann Rev Nuclear Particles Sci*, v 33, p 505–537.
- Shea, M A and Smart, D F, 1988, Cosmic ray and solar activity since 1955, *in* Cini Castagnoli, G, ed, *Solar-terrestrial relationships and the earth environment in the last millennia*, North Holland, Amsterdam: Internatl school of physics “Enrico Fermi,” Proc, p 396–407.
- Siegenthaler, U, Heimann, M and Oeschger, H, 1980, ^{14}C variations caused by changes in the global carbon cycle, *in* Stuiver, M and Kra, R S, eds, Internatl ^{14}C conf, 10th, Proc: *Radiocarbon*, v 22, no. 2, p 177–191.
- Sonett, C P, 1984, Very long solar periods and the radiocarbon record: *Rev Geophys Space Phys*, v 22, p 239–254.
- Sonett, C P and Suess, H E, 1986, A direct time series comparison between La Jolla and Belfast radiocarbon record, *in* Reedy, R C and Englert, P A J, Workshop on cosmogenic nuclides: LPI Tech rept 86–06, Lunar Planetary Inst, Houston, p 69–70.
- Storini, M, 1989, Galactic cosmic-ray modulation and solar terrestrial relationships: *Nuovo Cimento* v 17C, in press.
- Stuiver, M, (ms) 1988, Atmospheric ^{14}C change and oceanic variability: Paper presented at the 13th Internatl ^{14}C conf, Dubrovnik.
- Stuiver, M and Kra, R S, eds, 1986, Internatl ^{14}C conf, 12th, Proc: *Radiocarbon*, v 28, no. 2B.
- Stuiver, M and Quay, P D, 1980a, Patterns of atmospheric ^{14}C changes, *in* Stuiver, M and Kra, R S, eds, Internatl ^{14}C conf, 10th, Proc: *Radiocarbon*, v 22, no. 2, p 166–176.
- 1980b, Changes in atmospheric carbon-14 attributed to a variable sun: *Science*, v 207, no. 4426, p 11–19.
- 1981, Atmospheric ^{14}C changes resulting from fossil fuel CO_2 release and cosmic ray flux variability: *Earth Planetary Sci Letters*, v 53, p 349–362.
- Suess, H E, 1970, The three causes of secular ^{14}C fluctuations, their amplitudes and time constants, *in* Olsson, I U, ed, *Radiocarbon variations and absolute chronology*, Nobel symposium, 12th, Proc: New York, John Wiley & Sons, p 595–605.
- 1980a, Radiocarbon geophysics: *Endeavour*, ns v 4, no. 3, p 113–117.
- 1980b, The radiocarbon record in tree rings of the last 8000 years, *in* Stuiver, M and Kra, R S, eds, Internatl ^{14}C conf, 12th, Proc: *Radiocarbon*, v 22, no. 2, p 200–209.
- 1986, Secular variations of cosmogenic ^{14}C on earth: their discovery and interpretation, *in* Stuiver, M and Kra, R S, eds, Internatl ^{14}C conf, 12th, Proc: *Radiocarbon*, v 28, no. 2A, p 259–265.
- Wölfli, W, 1987, Advances in accelerator mass spectrometry: *Nuclear Instruments & Methods*, v B29, p 1–13.
- (ms) 1989, Archaeometry with accelerators: Paper presented at the 13th Internatl ^{14}C conf, Dubrovnik.